Preprints

2nd IFAC Workshop on Fractional Differentiation and its Applications

19 - 21 July, 2006
Porto, Portugal

Proceedings of the 2nd IFAC
Workshop on Fractional Differentiation and its Applications
Porto, Portugal, July 19-21, 2006

COMPARISON OF DIFFERENT ORDERS PADÉ FRACTIONAL ORDER PD$^{0.5}$ CONTROL ALGORITHM IMPLEMENTATIONS

Manuel F. Silva, J. A. Tenreiro Machado, Ramiro S. Barbosa

Department of Electrical Engineering, Institute of Engineering of Porto,
Rua Dr. António Bernardino de Almeida, 4200-072 Porto, Portugal
Email: {mss,jtm,rsb}@isep.ipp.pt

Abstract - This paper studies the performance of different order Padé Fractional Order (FO) PD$^{0.5}$ controllers applied to the leg joint control of a hexapod robot with two dof legs and joint actuators with saturation. For simulation purposes the robot prescribed motion is characterized through several locomotion variables and for the walking performance evaluation are used two indices, one based on the mean absolute density of energy per travelled distance and the other on the hip trajectory errors. A set of simulation experiments reveals the influence of the different order Padé PD$^{0.5}$ controllers tuning upon the proposed indices.

Keywords – Robotics, Locomotion, Control algorithms, Fractional-order control, Performance analysis

1. INTRODUCTION

Walking machines allow locomotion in terrain inaccessible to other type of vehicles, but the requirements for leg coordination and control impose difficulties beyond those encountered in wheeled robots. Previous studies focused mainly in the control at the leg level and leg coordination using different methods. In spite of the diversity of approaches, for multi-legged robots the control at the joint level is usually implemented through a simple PID like scheme with position / velocity feedback (Silva and Machado, 2005). Other approaches include sliding mode control, computed torque control and hybrid force / position control.

The application of the theory of fractional calculus in robotics is still in a research stage, but the recent progress in this area reveals promising aspects for future developments (Silva and Machado, 2005).

Taking into consideration these facts, a simulation model for multi-leg locomotion systems was developed, for several periodic gaits. This tool is adopted in the present study to evaluate the performance of different order Padé Fractional Order (FO) PD$^{0.5}$ control algorithms applied to the leg joint control of a hexapod robot. The analysis is based on the formulation of two indices measuring the mean absolute density of energy per travelled distance and the hip trajectory errors during walking.

Bearing these facts in mind, the paper is organized as follows. Section two introduces the robot kinematics and the motion planning scheme. Sections three and four present the robot dynamic model and control architecture, and the optimizing indices, respectively. Section five develops a set of simulation experiments to compare the performance of the different order Padé PD$^{0.5}$ controllers when applied to the hexapod joint leg control. Finally, section six outlines the main conclusions and some directions towards future developments.

2. ROBOT KINEMATICS AND TRAJECTORY PLANNING

We consider a walking system (Fig. 1) with $n = 6$ legs, equally distributed along both sides of the robot body, having each two rotational joints (*i.e.*, j = {1, 2} ≡ {hip, knee}) (Silva, *et al*., 2005). Motion is described by means of a world coordinate system. The kinematic model comprises: the cycle time T, the duty factor β, the transference time $t_T = (1-\beta)T$, the support time $t_S = \beta T$, the step length L_S, the stroke pitch S_P, the body height H_B, the maximum foot clearance F_C, the i^{th} leg lengths L_{i1} and L_{i2} and the i^{th} foot trajectory offset O_i. Moreover, we consider a periodic trajectory for each foot, with body velocity $V_F = L_S / T$.

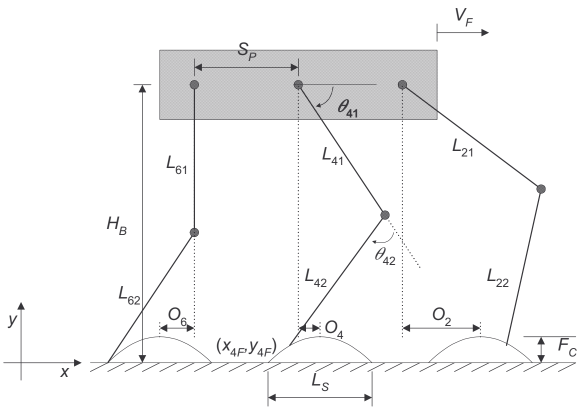

Fig. 1. Coordinate system and variables that characterize the motion trajectories of the multi-legged robot.

Gaits describe sequences of leg movements, alternating between transfer and support phases. Given a particular gait and duty factor β, it is possible to calculate, for leg i, the corresponding phase ϕ_i, the time instant where each leg leaves and returns to contact with the ground and the cartesian trajectories of the tip of the feet (that must be completed during t_T). Based on this data, the trajectory generator is responsible for producing a motion that synchronises and coordinates the legs.

The robot body, and by consequence the legs hips, is assumed to have a desired horizontal movement with a constant forward speed V_F. Therefore, for leg i the cartesian coordinates of the hip of the legs are given by $\mathbf{p_{Hd}}(t) = [x_{iHd}(t), y_{iHd}(t)]^{\mathrm{T}}$:

$$\mathbf{p_{Hd}}(t) = \left[V_F t - S_p\left(\mathrm{ceil}(i/2) - 1\right) \quad H_B\right]^{\mathrm{T}} \tag{1}$$

Regarding the feet trajectories, on a previous work we evaluated two alternative space-time foot trajectories, namely a cycloidal and a sinusoidal function (Silva, *et al*., 2003). It was demonstrated that the cycloid is superior to the sinusoidal function, since it improves the hip and foot trajectory tracking, while minimising the corresponding joint torques. However, a step acceleration profile is assumed for the feet trajectories. These results do not present significant changes for different acceleration profiles of the foot trajectory.

In order to avoid the impact and friction effects, at the planning phase we impose null velocities of the feet in the instants of landing and taking off, assuring also the velocity continuity.

Considering the above conclusions, for each cycle the desired geometric trajectory of the foot of the swing leg is computed through a cycloid function (Eq. 2). For example, considering that the transfer phase starts at $t = 0$ s for leg $i = 1$ we have for $\mathbf{p_{Fd}}(t) = [x_{iFd}(t), y_{iFd}(t)]^{\mathrm{T}}$:

- during the transfer phase:

$$\mathbf{p_{Fd}}(t) = \left[V_F\left[t - \frac{t_T}{2\pi}\sin\left(\frac{2\pi t}{t_T}\right)\right], \ \frac{F_C}{2}\left[1 - \cos\left(\frac{2\pi t}{t_T}\right)\right]\right]^{\mathrm{T}} \tag{2}$$

- during the stance phase:

$$\mathbf{p_{Fd}}(t) = \left[V_F T \quad 0\right]^{\mathrm{T}} \tag{3}$$

The algorithm for the forward motion planning accepts the desired cartesian trajectories of the leg hips $\mathbf{p_{Hd}}(t)$ and feet $\mathbf{p_{Fd}}(t)$ as inputs and, by means of an inverse kinematics algorithm ψ^{-1}, generates the related joint trajectories $\mathbf{\Theta_d}(t) = [\theta_{i1d}(t), \theta_{i2d}(t)]^{\mathrm{T}}$, selecting the solution corresponding to a forward knee:

$$\mathbf{p_d}(t) = \left[x_{id}(t) \quad y_{id}(t)\right]^{\mathrm{T}} = \mathbf{p_{Fd}}(t) - \mathbf{p_{Hd}}(t) \tag{4a}$$

$$\mathbf{p_d}(t) = \psi\left[\mathbf{\Theta_d}(t)\right] \Rightarrow \mathbf{\Theta_d}(t) = \psi^{-1}\left[\mathbf{p_d}(t)\right] \tag{4b}$$

$$\dot{\mathbf{\Theta}}_{\mathbf{d}}(t) = \mathbf{J}^{-1}\left[\dot{\mathbf{p}}_{\mathbf{d}}(t)\right], \ \mathbf{J} = \frac{\partial\psi}{\partial\mathbf{\Theta_d}} \tag{4c}$$

3. ROBOT DYNAMICS AND CONTROL ARCHITECTURE

3.1 Inverse Dynamics Computation

The planned joint trajectories constitute the reference for the robot control system. The model for the robot inverse dynamics is formulated as:

$$\mathbf{\Gamma} = \mathbf{H}(\mathbf{\Theta})\ddot{\mathbf{\Theta}} + \mathbf{c}\left(\mathbf{\Theta}, \dot{\mathbf{\Theta}}\right) + \mathbf{g}(\mathbf{\Theta}) - \mathbf{F_{RH}} + \mathbf{J_F^T}(\mathbf{\Theta})\mathbf{F_{RF}} \tag{5}$$

where $\mathbf{\Gamma} = [f_{ix}, f_{iy}, \tau_{i1}, \tau_{i2}]^{\mathrm{T}}$ ($i = 1, \ldots, n$) is the vector of forces/torques, $\mathbf{\Theta} = [x_{iH}, y_{iH}, \theta_{i1}, \theta_{i2}]^{\mathrm{T}}$ is the vector of position coordinates, $\mathbf{H}(\mathbf{\Theta})$ is the inertia matrix and $\mathbf{c}\left(\mathbf{\Theta}, \dot{\mathbf{\Theta}}\right)$ and $\mathbf{g}(\mathbf{\Theta})$ are the vectors of centrifugal/Coriolis and gravitational forces/torques, respectively. The $n \times m$ ($m = 2$) matrix $\mathbf{J_F^T}(\mathbf{\Theta})$ is the transpose of the robot Jacobian matrix, $\mathbf{F_{RH}}$ is the $m \times 1$ vector of the body inter-segment forces and $\mathbf{F_{RF}}$ is the $m \times 1$ vector of the reaction forces that the ground exerts on the robot feet. These forces are null during the foot transfer phase. During the system simulation, Eq. (5) is integrated through the Runge-Kutta method.

We consider that the joint actuators are not ideal, exhibiting a saturation given by:

$$\tau_{ijm} = \begin{cases} \tau_{ijC} & , \ \left|\tau_{ijm}\right| \le \tau_{ijMax} \\ \mathrm{sgn}\left(\tau_{ijC}\right) \cdot \tau_{ijMax} & , \ \left|\tau_{ijm}\right| > \tau_{ijMax} \end{cases} \tag{6}$$

where, for leg i and joint j, τ_{ijC} is the controller demanded torque, τ_{ijMax} is the maximum torque that the actuator can supply and τ_{ijm} is the motor effective torque.

3.2 Robot Body Model

Figure 2 presents the dynamic model for the hexapod body and foot-ground interaction. It is considered robot body compliance because walking animals have a spine that allows supporting the locomotion with improved stability. In the present study, the robot body is divided in n identical segments (each with mass $M_b n^{-1}$) and a linear spring-damper system is adopted to implement the intra-body compliance:

$$f_{i\eta H} = -\sum_{i'=1}^{u} \left[K_{\eta H} \left(\eta_{iH} - \eta_{i'H} \right) + B_{\eta H} \left(\dot{\eta}_{iH} - \dot{\eta}_{i'H} \right) \right] \tag{7}$$

where $(x_{i'H}, y_{i'H})$ are the hip coordinates and u is the total number of segments adjacent to leg i.

In this study, the parameters $K_{\eta H}$ and $B_{\eta H}$ ($\eta = \{x, y\}$) in the {horizontal, vertical} directions, respectively, are defined so that the body behaviour is similar to the one expected to occur on an animal (Table 1).

3.3 Foot-Ground Interaction Model

The contact of the i^{th} robot feet with the ground is modelled through a non-linear system (Silva, *et al.*, 2005) with linear stiffness $K_{\eta F}$ and non-linear damping $B_{\eta F}$ ($\eta = \{x, y\}$) in the {horizontal, vertical} directions, respectively (see Fig. 2), yielding:

$$f_{i\eta F} = -K_{\eta F} \left(\eta_{iF} - \eta_{iF0} \right) - B_{\eta F} \left[-\left(y_{iF} - y_{iF0} \right) \right]^{v_\eta} \left(\dot{\eta}_{iF} - \dot{\eta}_{iF0} \right)$$
$$v_x = 1.0,\ v_y = 0.9 \tag{8}$$

where x_{iF0} and y_{iF0} are the coordinates of foot i touchdown and v_η ($\eta = \{x, y\}$) is a parameter dependent on the ground characteristics. The values for the parameters $K_{\eta F}$ and $B_{\eta F}$ (Table 1) are based on the studies of soil mechanics (Silva, *et al.*, 2003).

3.4 Control Architecture

The general control architecture of the hexapod robot is presented in Fig. 3. On a previous work were demonstrated the advantages of a cascade controller, with PD position control and foot force feedback, over a classical PD with, merely, position feedback, particularly in real situations where we have non-ideal actuators with saturation and being also more robust for variable ground characteristics (Silva, *et al.*, 2003). Previous studies have also allowed us to conclude that the control of a hexapod walking robot through a FO PD$^{\alpha}$ algorithm guaranteed the best performance for the fractional order $\alpha_j = 0.5$ (Silva and Machado, 2005). Based on these results, we now evaluate the effect of different orders of the FO PD$^{0.5}$ controller adopted for $G_{c1}(s)$, while for G_{c2} it is considered a simple P controller. For the FO PD$^{\alpha}$ algorithm we have:

$$G_{C1j}(s) = Kp_j + K\alpha_j s^{\alpha_j},\quad \alpha_j \in \Re,\quad j = 1, 2 \tag{9}$$

where Kp_j and $K\alpha_j$ are the proportional and derivative gains, respectively, and α_j is the fractional order, for joint j.

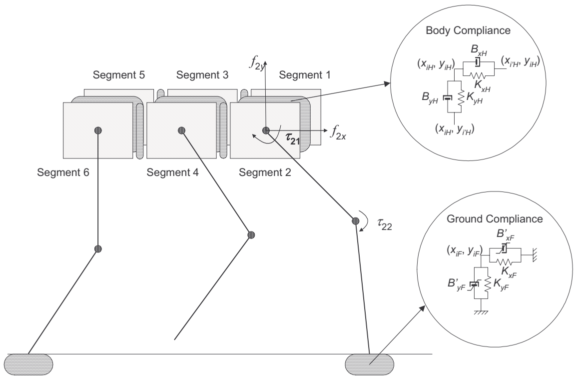

Fig. 2. Model of the robot body and foot-ground interaction.

Table 1 System parameters

Robot model parameters		Locomotion parameters	
S_P	1 m	β	50%
L_{ij}, j=1,2	0.5 m	L_S	1 m
L_{i3}	0.1 m	H_B	0.9 m
O_i	0 m	F_C	0.1 m
M_b	88.0 kg	V_F	1 ms^{-1}
M_{ij}, j=1,2	1 kg	**Ground parameters**	
M_{i3}	0.1 kg	K_{xF}	1.3×10^6 Nm^{-1}
K_{xH}	10^5 Nm^{-1}	K_{yF}	1.7×10^6 Nm^{-1}
K_{yH}	10^4 Nm^{-1}	B_{xF}	2.3×10^6 Nsm^{-1}
B_{xH}	10^3 Nsm^{-1}	B_{yF}	2.7×10^6 Nsm^{-1}
B_{yH}	10^2 Nsm^{-1}		

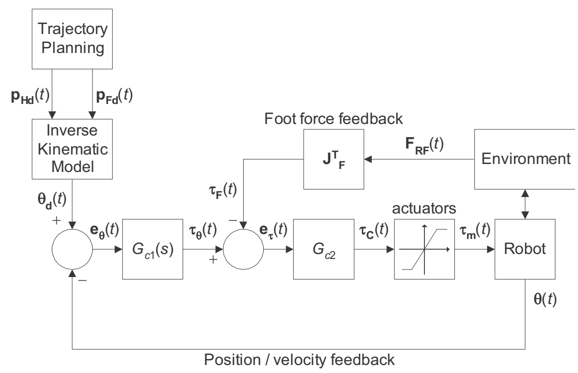

Fig. 3. Hexapod robot control architecture.

In this paper, for implementing the FO algorithm (Eq. (9)) it is adopted a discrete-time u^{th}-order Padé approximation (a_{ij}, $b_{ij} \in \Re$, $j = 1, 2$) yielding an equation in the z-domain of the type:

$$G_{C1j}(z) \approx Kp_j + K\alpha_j \sum_{i=0}^{i=u} a_{ij} z^{-i} \Big/ \sum_{i=0}^{i=u} b_{ij} z^{-i}. \tag{10}$$

4. MEASURES FOR PERFORMANCE EVALUATION

In mathematical terms we establish two global measures of the overall performance of the mechanism in an average sense. In this perspective, we define one index $\{E_{av}\}$ inspired on the system dynamics and another one $\{\varepsilon_{xyH}\}$ based on the trajectory tracking errors.

Regarding the mean absolute density of energy per travelled distance E_{av}, it is computed assuming that energy regeneration is not available by actuators doing negative work (by taking the absolute value of the power). At a given joint j (each leg has $m = 3$ joints) and leg i (since we are adopting a hexapod it yields $n = 6$ legs), the mechanical power is the product of the motor torque and angular velocity. The global index E_{av} is obtained by averaging the mechanical absolute energy delivered over the travelled distance d:

$$E_{av} = \frac{1}{d}\sum_{i=1}^{n}\sum_{j=1}^{m}\int_0^T \left|\tau_{ij}(t)\,\dot{\theta}_{ij}(t)\right| dt \quad \left[\mathrm{Jm}^{-1}\right] \tag{11}$$

In what concerns the hip trajectory following errors we can define the index:

$$\varepsilon_{xyH} = \sum_{i=1}^{n}\sqrt{\frac{1}{N_s}\sum_{k=1}^{N_s}\left(\Delta_{ixH}^2 + \Delta_{iyH}^2\right)} \quad [\mathrm{m}]$$
$$\Delta_{ixH} = x_{iHd}(k) - x_{iH}(k), \quad \Delta_{iyH} = y_{iHd}(k) - y_{iH}(k) \tag{12}$$

where N_s is the total number of samples for averaging purposes and $\{d, r\}$ indicate the i^{th} samples of the desired and real position, respectively.

In all cases the performance optimization requires the minimization of each index.

5. SIMULATION RESULTS

In this section we develop a set of simulations to analyse the performances of the different orders of the FO PD$^{0.5}$ controller during a periodic wave gait at a constant forward velocity V_F. For simulation purposes we consider the locomotion parameters, the robot body parameters and the ground parameters (supposing that the robot is walking on a ground of compact clay) presented in Table 1.

To tune the different controller implementations we adopt a systematic method, testing and evaluating a narrow grid of several possible combinations of parameters, for all controller implementations. Namely, we vary the controller gains in the intervals $0.0 \le Kp_j \le 10^5$ and $0.0 \le K\alpha_j \le 10^5$. Moreover, it is assumed high performance joint actuators, with a maximum actuator torque in Eq. (6) of $\tau_{ijMax} = 400$ Nm and a proportional controller G_{c2} with gain $Kp_j = 0.9$ ($j = 1, 2$).

Each dot in the charts of Figure 4 depicts the results of a particular $G_{c1}(s)$ controller tuning ($\{Kp_j, K\alpha_j\}$), in terms of $\{E_{av}, \varepsilon_{xyH}\}$ for different orders u ($u = \{1, 2, 4, 6, 13\}$) of the Padé approximation.

We conclude that for the orders $u = 0$ and $u > 14$ there is no $G_{c1}(s)$ controller tuning that allows the locomotion to be performed with the performance measures on the ranges $0.5 \le \varepsilon_{xyH} \le 3.0$ and $350.0 \le E_{av} \le 600.0$. For values such that $1 \le u \le 13$ we have several different tunings allowing the locomotion to be performed inside these performance measures ranges.

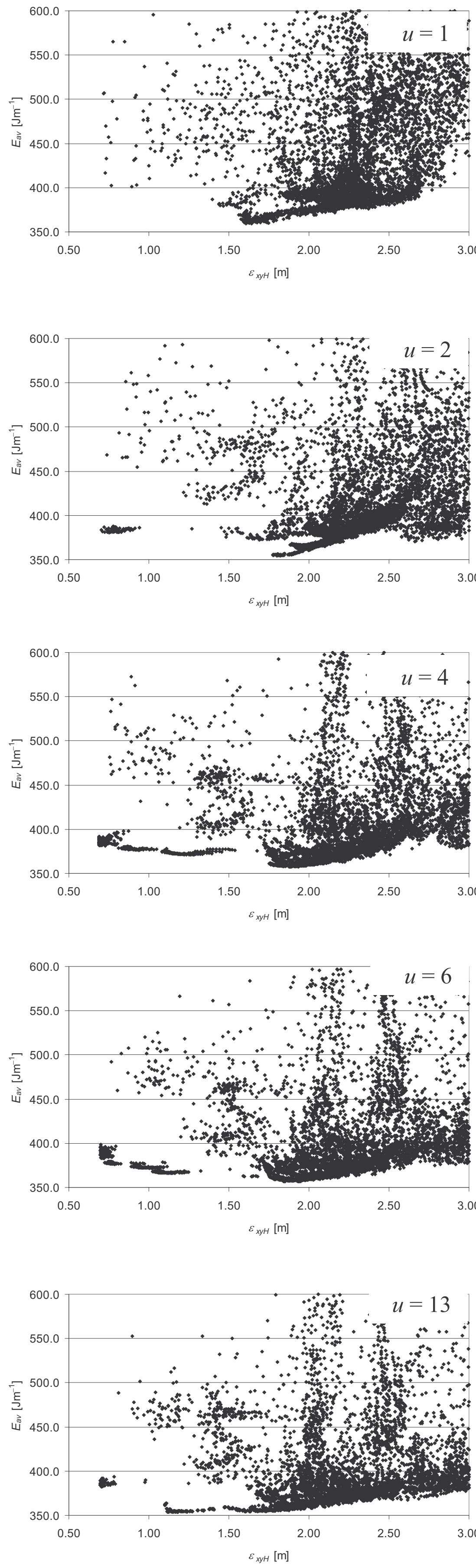

Fig. 4. Plots of ε_{xyH} *vs.* E_{av} for different number of terms ($u = \{1, 2, 4, 6, 13\}$) of the Padé approximation for the PD$^{0.5}$ $G_{c1}(s)$, with $G_{c2} = 0.9$.

From the observation of Figure 4, it is concluded that for the Padé order u = 1 there is no $G_{c1}(s)$ controller tuning that allows the locomotion to be performed with simultaneous low hip trajectory tracking errors ($\varepsilon_{xyH} \leq 1.0$) and low energy consumption ($E_{av} \leq 400.0$).

For increasing orders u, the number of possible $G_{c1}(s)$ controller tuning, that allows the locomotion to be performed with simultaneous low values for ε_{xyH} and E_{av}, increases until $u \approx 6$. For higher Padé orders $7 \leq u \leq 13$ this number starts to decrease again. Finally, as previously stated, for $u \approx 14$ the number of "good" solutions becomes zero.

This first analysis, based solely on the possible number of "good" solutions, might lead us to state that, for this application of the $PD^{0.5}$ controller, it is best to use a Padé approximation with $3 \leq u \leq 6$. In the sequel we are going to analyse the best solution when it is chosen taking into account only the minimization of the performance measure ε_{xyH}, only the minimization of the index E_{av} or a compromise for the simultaneous minimization of ε_{xyH} and E_{av}.

Table 2 presents the best $G_{c1}(s)$ controller tuning for different orders of the Padé approximation, when considering the best solution as the one that presents the minimum value of ε_{xyH}. We conclude that the best solution corresponds to the Padé order u = 4, followed by the Padé orders u = 3 and u = 5. Moreover, for $2 \leq u \leq 13$ the results remain very similar, both in terms of ε_{xyH} and E_{av}.

Following we analyse the best $G_{c1}(s)$ controller tuning for different values of u, when considering the best solution as the one that presents the minimum value of E_{av}. We conclude, from the analysis of Table 3, that the best solution corresponds to the Padé order u = 13. From the observation of the same table, we conclude that for $2 \leq u \leq 13$ the results remain very similar, both in terms of ε_{xyH} and E_{av}.

Finally, we analyse the best locomotion performance, for distinct values u of the Padé approximation for the $G_{c1}(s)$ control algorithm, while considering that the best solution corresponds to a compromise between the simultaneous minimization of ε_{xyH} and E_{av}. From this viewpoint, we conclude that the best solutions correspond to the Padé orders $3 \leq u \leq 9$ (Table 4). Outside these values there is a clear degradation of the hexapod locomotion performance, more pronounced for the Padé approximations of orders u = 0 and u = 14.

It is worth mentioning that another criterion to be considered when choosing the Padé order for a practical implementation is the required computation power. From this viewpoint, low order Padé approximations are preferred. Therefore, and considering all the previous results, we may state that the best order for the Padé approximation when computing the $G_{c1}(s)$ algorithm yields for $u \approx 4$.

Table 2 Minimum values of ε_{xyH}, and the corresponding values of E_{av}, for different number of terms u of the Padé approximation for the $PD^{0.5}$ $G_{c1}(s)$ controller, with G_{c2} = 0.9

u	ε_{xyH}	E_{av}	Kp_1	Kp_2	$K\alpha_1$	$K\alpha_2$
0	1.647	2210.305	4000.0	1000.0	0.0	0.0
1	0.718	506.752	9000.0	5000.0	4500.0	0.0
2	0.703	383.916	10000.0	4000.0	9500.0	0.0
3	0.692	380.852	10000.0	1000.0	8000.0	500.0
4	0.688	390.432	6000.0	2000.0	10000.0	500.0
5	0.695	386.954	7000.0	4000.0	9500.0	0.0
6	0.696	395.448	10000.0	4000.0	9500.0	0.0
7	0.696	386.657	10000.0	4000.0	9500.0	0.0
8	0.696	395.305	6000.0	4000.0	9000.0	0.0
9	0.697	386.919	5000.0	4000.0	9000.0	0.0
10	0.697	387.293	5000.0	4000.0	9000.0	0.0
11	0.697	389.391	7000.0	4000.0	9000.0	0.0
12	0.697	387.966	7000.0	4000.0	9000.0	0.0
13	0.697	384.518	10000.0	4000.0	9000.0	0.0
14	2.342	896.129	3000.0	1000.0	0.0	0.0

Table 3 Minimum values of E_{av}, and the corresponding values of ε_{xyH}, for different number of terms u of the Padé approximation for the $PD^{0.5}$ $G_{c1}(s)$ controller, with G_{c2} = 0.9

u	ε_{xyH}	E_{av}	Kp_1	Kp_2	$K\alpha_1$	$K\alpha_2$
0	2.342	896.129	3000.0	1000.0	0.0	0.0
1	1.605	359.444	1000.0	1000.0	9500.0	500.0
2	1.801	354.620	9000.0	1000.0	9000.0	500.0
3	1.854	356.922	5000.0	2000.0	8000.0	500.0
4	1.874	357.603	10000.0	3000.0	7000.0	500.0
5	1.782	357.604	0.0	2000.0	6500.0	500.0
6	1.852	356.767	0.0	2000.0	6500.0	500.0
7	1.823	355.104	0.0	0.0	5500.0	500.0
8	1.683	354.495	5000.0	0.0	6000.0	500.0
9	1.509	354.469	2000.0	0.0	7000.0	500.0
10	1.772	354.338	0.0	1000.0	6500.0	500.0
11	1.752	354.901	0.0	1000.0	6500.0	500.0
12	1.729	354.844	5000.0	2000.0	7000.0	500.0
13	1.182	353.694	0.0	0.0	7500.0	500.0
14	3.292	1051.539	5000.0	1000.0	0.0	0.0

Table 4 Best compromise situation in terms of the simultaneous minimization of ε_{xyH} and E_{av}, for different number of terms u of the Padé approximation for the $PD^{0.5}$ $G_{c1}(s)$ controller, with G_{c2} = 0.9

u	ε_{xyH}	E_{av}	Kp_1	Kp_2	$K\alpha_1$	$K\alpha_2$
0	2.342	896.129	3000.0	1000.0	0.0	0.0
1	0.765	402.417	0.0	4000.0	10000.0	0.0
2	0.712	381.752	8000.0	4000.0	9500.0	0.0
3	0.705	378.329	9000.0	1000.0	7000.0	500.0
4	0.693	381.761	7000.0	2000.0	6500.0	500.0
5	0.700	379.140	10000.0	2000.0	7500.0	500.0
6	0.723	378.022	5000.0	2000.0	7500.0	500.0
7	0.718	378.770	10000.0	2000.0	7500.0	500.0
8	0.773	369.837	3000.0	0.0	10000.0	500.0
9	0.753	369.331	3000.0	0.0	7500.0	500.0
10	0.726	375.215	8000.0	1000.0	8000.0	500.0
11	0.720	374.603	0.0	1000.0	7500.0	500.0
12	0.722	374.091	0.0	1000.0	7000.0	500.0
13	0.703	382.705	3000.0	4000.0	9000.0	0.0
14	2.342	896.129	3000.0	1000.0	0.0	0.0

In Figures 5 and 6 are depicted the joint actuation torques τ_{1jm} and the hip trajectory tracking errors Δ_{1xF}, along one robot locomotion step, considering a Padé approximation for the $PD^{0.5}$ $G_{c1}(s)$ controller with four terms (u = 4) and G_{c2} = 0.9.

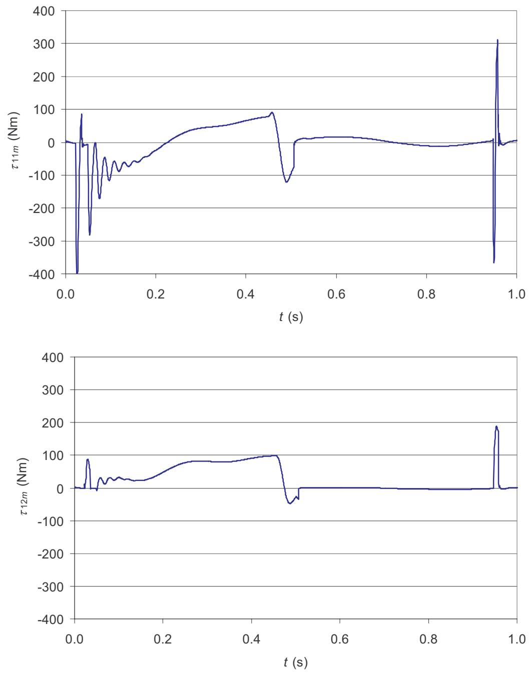

Fig. 5. Plots of τ_{1jm} *vs*. t, considering a Padé approximation for the PD$^{0.5}$ $G_{c1}(s)$ with four terms ($u = 4$) and $G_{c2} = 0.9$.

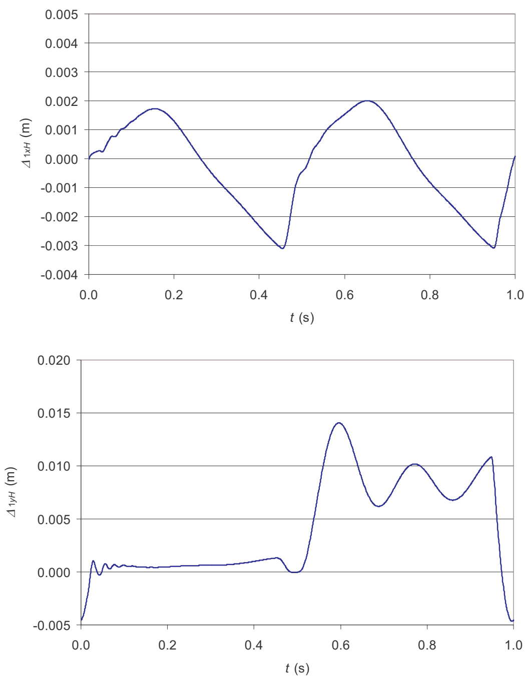

Fig. 6. Plots of Δ_{1xH} and Δ_{1yH} *vs*. t, considering a Padé approximation for the PD$^{0.5}$ $G_{c1}(s)$ with four terms ($u = 4$) and $G_{c2} = 0.9$.

From the analysis of these figures it is possible to conclude that, for the algorithm implementation with this Padé order (according to the previous studies), the robot locomotion is performed with only minor oscillations in the hip joint torque, largely due to the feet impact with the ground at the end of the transfer phase, and with much lower oscillations in the knee torque. Furthermore, it is possible to conclude that the torque that the actuators must supply along the locomotion cycle is lower than the actuators saturation torque, as desirable.

Finally, looking into the charts of Figure 6 it is possible to conclude that the errors introduced along the walking robot locomotion cycle are almost negligible in the x direction, meaning that the controller allows to correctly following the planned trajectory. Along the y direction, however, it is seen a relatively large trajectory following error during half of the robot locomotion cycle ($0.5 \leq t \leq 1$ s), that corresponds to the support phase on which the robot has this leg on the ground helping support the robot body. This leads to large efforts on this leg, and correspondingly to the large hip trajectory tracking errors.

6. CONCLUSIONS

In this paper we have compared the performance of different order Padé FO PD$^{0.5}$ controllers applied to the leg joint control of a hexapod robot with two dof legs and leg joint actuators having saturation.

In order to analyze the system performance two measures were defined, the first based on the mean absolute density of energy per travelled distance and the second on the hip trajectory errors.

The simulation experiments reveal that the PD$^{0.5}$ controller implementation using the Padé approximation with a small number of terms ($3 < u < 6$) gives the best results, both in terms of the high possible number of good solutions and in terms of the solution with simultaneous low values for E_{av} and ε_{xyH}.

The focus of the work presented has been on the use of the Padé approximation for the implementation of the PD$^{0.5}$ controllers with a proportional plus a derivative / integrative term. Presently we are studying the performance of the system in case we use the series approximation for the implementation of the FO PD$^{0.5}$. Future work in this area will also address the study of the performance of a FO PID control algorithm of the type PI$^{\lambda}$D$^{\alpha}$ and the study of complex-order control algorithms.

REFERENCES

Silva, M. F. and Machado, J. A. T. (2005). Integer vs. Fractional Order Control of a Hexapod Robot, in *Climbing and Walking Robots*, Manuel A. Armada and Pablo Gonzaléz de Santos (Eds.), Springer, pp. 73–83.

Silva, M. F., Machado, J. A. T. and Barbosa, R. S. (2006). Complex-Order Dynamics in Hexapod Locomotion, *Signal Processing*. Accepted for publication.

Silva, M. F., Machado, J. A. T. and Lopes, A. M. (2003). Position / Force Control of a Walking Robot. *MIROC –Machine Intelligence and Robot Control*, **5**, pp. 33 – 44.

Silva, M. F., Machado, J. A. T. and Lopes, A. M. (2005). Modelling and Simulation of Artificial Locomotion Systems, *ROBOTICA*, **23**, pp. 595 – 606.